Materials Science and Engineering C 33 (2013) 3677–3687

Contents lists available at ScienceDirect

Materials Science and Engineering C

journal homepage: www.elsevier.com/locate/msec

Biomimetic poly(glycerol sebacate) (PGS) membranes for cardiac patch application

Ranjana Rai [a], Marwa Tallawi [a], Niccoletta Barbani [b], Caterina Frati [c], Denise Madeddu [c], Stefano Cavalli [c], Gallia Graiani [c], Federico Quaini [c], Judith A. Roether [d], Dirk W. Schubert [d], Elisabetta Rosellini [b,*], Aldo R. Boccaccini [a,**]

[a] Institute of Biomaterials, Department of Materials Science and Engineering, University of Erlangen-Nuremberg, 91058 Erlangen, Germany
[b] Department of Chemical Engineering, Industrial Chemistry and Materials Science, Largo Lucio Lazzarino, 56126 Pisa, Italy
[c] Department of Medicine and Pathology, University of Parma, 12-I 43126 Parma, Italy
[d] Institute of Polymeric Materials, Department of Materials Science and Engineering, University of Erlangen-Nuremberg, 91058 Erlangen, Germany

ARTICLE INFO

Article history:
Received 16 January 2013
Received in revised form 12 April 2013
Accepted 26 April 2013
Available online 4 May 2013

Keywords:
Poly(glycerol sebacate)
Cardiac patch
Biomimetic
Surface modification
Laminin
Fibronectin

ABSTRACT

In this study biomimetic poly(glycerol sebacate) PGS matrix was developed for cardiac patch application. The rationale was that such matrices would provide conducive environment for the seeded cells at the interphase with PGS. From the microstructural standpoint, PGS was fabricated into dense films and porous PGS scaffolds. From the biological aspect, biomimetic PGS membranes were developed via covalently binding peptides Tyr-Ile-Gly-Ser-Arg (YIGSR) and Gly-Arg-Gly-Asp-Ser-Pro (GRGDSP), corresponding to the epitope sequences of laminin and fibronectin, respectively onto the surface. To improve and enhance homogenous binding of peptides onto the PGS surface, chemical modification of its surface was carried out. A sequential regime of alkaline hydrolysis with 0.01 M NaOH for 5 min and acidification with 0.01 M HCl for 25 s was optimal. More COOH chemical group was exposed without causing deleterious effect on the bulk properties of the polymer as revealed by the physicochemical analysis carried out. HPLC analysis, chemical imaging and ToF-SIMS were able to establish the successful homogenous functionalization of PGS membranes with the peptides. Finally, the developed biomimetic membranes supported the adhesion and growth of rat and human cardiac progenitor cells.

1. Introduction

Cardiovascular diseases CVDs are the number one cause of death globally [1]. People die more annually from CVDs than from any other cause. By 2030, almost 23.6 million people will die from CVDs, mainly from heart disease and stroke [1]. These are projected to remain the single leading cause of death. Myocardial infarction (or heart attack) is one of the major causes of death in patients suffering from CVD [1].

A biphasic ischemic/reperfusion injury occurs after coronary artery occlusion. First, cardiomyocytes die resulting in a significant loss of functioning muscle mass [2,3] and this is followed by a second wave of inflammation based tissue damage. The adult heart cannot repair the damaged tissue, as the mature contracting cardiomyocytes possess a limited proliferative capacity [4,5]. Therefore, fibrous noncontractile scar replaces the ischemic myocardial region of the ventricle constituting the infarcted area. The scar does not effectively conduct the electro-mechanical wave front, reducing left ventricular (LV) performance which further leads to increased wall stress in the remaining viable myocardium [2,3]. This process, brought about by a sequence of molecular, cellular, and physiological events results in LV dilation and ultimately leads to end stage congestive heart failure (CHF) [6,7]. Besides poorly efficient pharmacological interventions, current available treatments for CHF are cardiac transplantation and the use of ventricular assist devices (VADs). However, these treatments are besieged with acute problems of donor heart scarcity and high cost of VADs. It is in this context, that research on regenerative approaches for engineering cardiac tissues to treat myocardial infarction has been gaining momentum. One such approach is the 'cardiac patch' approach. Here, matrices or scaffolds are designed in order to be populated by relevant cells and to develop a viable cardiac construct that can be patched onto the infarcted region of the heart. The cardiac patch therefore aims to achieve a twofold objective i.e. first to deliver healthy cardiac cells to the injured infarcted myocardium and second to provide mechanical support to the infarcted ventricle.

In this respect, research is taking place to exploit the native features of extracellular matrix (ECM) for implementation in tissue engineering approaches. The ECM components play a central role in growth and

* Corresponding author. Tel.: +49 913185 20806; fax: +49 9131 85 28602.
** Corresponding author. Tel.: +49 9131 85 28601; fax: +49 9131 85 28602.
E-mail addresses: elisabetta.rosellini@diccism.unipi.it (E. Rosellini), aldo.boccaccin@ww.uni-erlangen.de (A.R. Boccaccini).

0928-4931
http://dx.doi.org/10.1016/j.msec.2013.04.058

development of tissues [8]. Extensive research is now currently taking place in designing and developing biomimetic materials to generate three dimensional scaffolds that mimic native ECM. Thus, efforts have been made to produce biomaterials matching native ECM biomechanical properties and supporting cell functions such as adhesion, growth, differentiation and the expression of tissue specific genes. ECM, in addition to functionally supporting the tissues, holds a plethora of information needed for each specific tissue cell subtype. The information is provided in the form of specific chemical signals from peptide epitopes contained in a wide variety of extracellular matrix molecules such as laminins and fibronectin. These peptide epitopes provide the chemical cues/signals for cell–matrix interaction via integrin recognition and thus play an important role in mediating and regulating the cellular behavior such as growth, differentiation, adhesion and motility [9]. Owing to these contentions, an approach has been to coat or covalently bind such integrin binding epitopes on the surface of the designed biomaterial [10,11].

In this study biomimetic polyglycerol sebacate (PGS) membranes were developed as cardiac patches for the treatment of myocardial infarction. PGS, a synthetic polyester, is prepared by polycondensing glycerol and sebacic acid. Sebacic acid is the natural metabolic intermediate in ω-oxidation of medium- to long-chain fatty acids [12–16] and has been shown to be safe in vivo [16,17]. The US Food and Drug Administration (FDA) has approved glycerol to be used as humectant in foods, and polymers containing sebacic acid, e.g. polifeprosan has been approved for medical applications like drug delivery [16,18]. As a result PGS is a biocompatible and a bioresorbable polymer. It is also an inexpensive polymer with tailorable mechanical properties and degradation kinetics that could be targeted to a particular application. It is because of these positive attributes that PGS is increasingly being studied for cardiac tissue engineering applications [19]. However, until now only one such investigation has been carried out in developing biomimetic surfaces of PGS membranes using peptide epitope sequences of the ECM macromolecules for tissue engineering applications [20]. In the study carried out by Pritchard et al. [20] the surface of PGS membranes was functionalized with peptides containing the RGD sequence, GRGDS for retinal transplantation. Other studies of modifying PGS surfaces have involved coating of the surface with ECM macromolecules such as laminin, fibronectin, fibrin, collagen type I/III and elastin [21].

Therefore, the main aim of this study was to develop biomimetic PGS membranes containing peptide sequences able to function as a cell delivery vehicle to supply healthy cardiac cells to the infarcted myocardium and also left ventricular restrain. Two different biomimetic PGS membranes were developed by covalently binding the peptides, containing the sequences Tyr-Ile-Gly-Ser-Arg (YIGSR) and Gly-Arg-Gly-Asp-Ser-Pro (GRGDSP), corresponding to the epitope sequences of laminin and fibronectin, respectively onto the surface. Laminin and fibronectin are amongst the two vital biomacromolecules present in the ECM. For the development of the biomimetic PGS membranes, modification of PGS was first carried out to expose COOH functional groups on its surface. This was achieved by sequential alkaline hydrolysis and acidification of the PGS membrane. To this modified PGS surface, the peptides YIGSR and GRGDSP were then covalently attached. To the authors' knowledge this is the first time that such an approach of chemical modification of PGS surface and subsequent covalent attachment of peptides onto the chemically modified PGS surface has been carried out. The developed biomimetic PGS membranes were also subjected to in vitro biocompatibility assessment using human cardiac mesenchymal stem cells (hC-MSCs) and rat cardiac progenitor cells (rCPCs).

2. Materials and methods

2.1. Materials

The chemicals were obtained from Sigma-Aldrich or VWR Ltd. unless otherwise stated. Analytical studies were carried out using analytical grade reagents. Chromatography grade reagents were used for high performance liquid chromatography (HPLC) study. The peptide sequences chosen for functionalization were synthesized in Cambridge Research Biochemicals, UK, introducing a spacer made by three residues of glycine, (i.e. GGG-GRGDSP and GGG-YIGSR) in order to provide more flexibility and to promote their interactions with the integrin receptors.

2.2. Synthesis of polyglycerol sebacate) (PGS)

The synthesis of PGS was carried out as described by Wang et al. [16] with slight adaptation of the reaction parameters. The synthesis involved two steps: (1) pre-polycondensation step and (2) crosslinking. For the pre-polycondensation step, an equimolar mixture (0.1 M) of glycerol (Sigma Aldrich, Germany) and sebacic acid (Sigma Aldrich, Germany) was heated at 120 °C under inert nitrogen atmosphere to form the pre-polycondensed polymer. The pre-polycondensed polymer was a transparent viscous liquid. Following this, the crosslinking step was carried out also at 120 °C and under a vacuum level of 1.3 to 2.5×10^{-2} mTorr for 4 days. The final crosslinked polymer produced was a transparent film.

2.3. Fabrication of two dimensional, (2D) dense and 2D porous PGS films

Fabrication of the desired 2D PGS dense films was carried out via solvent casting followed by crosslinking. Required amount of prepolymer corresponding to the required thickness (>1 mm) of the final fabricated PGS film was determined using the following equations:

$$\text{Volume} = \pi r^2 h \tag{1}$$

$$\rho = m/v. \tag{2}$$

From Eqs. (1) and (2) the mass of prepolymer used for obtaining the desired PGS thickness was calculated. The desired amount of the prepolymer (2 g) was dissolved in dimethylcarbonate (DMC) and then casted into the Teflon molds (55 mm diameter). Following complete removal of the solvent, the films were then crosslinked for 4 days at 120 °C and vacuum level of 1.3 to 2.5×10^{-2} mTorr.

Fabrication of porous PGS scaffold was carried out using the salt leaching method. A bed of NaCl salt particles was first prepared in a Teflon mold of 55 mm in diameter. Required amount of salt corresponding to the required thickness (>1 mm) of the final fabricated PGS film was again determined using the above Eqs. (1) and (2). The required salt was then used for preparing a salt bed in the mold. To this prepared salt bed, PGS prepolymer was introduced and subjected to crosslinking for 4 days at a vacuum level of 1.4×10^{-2} mTorr. Once the crosslinking was over, the salt particles were leached out by immersing the film in distilled water. Washing was continued until no increase in pH was observed in the distilled water in which the films were immersed for salt leaching, indicating that all the salt particles have been leached out. The washed films were then subjected to lyophilization followed by freeze drying.

2.4. Molar mass analysis

The molar mass of the PGS prepolymer was determined by carrying out Gel Permeation Chromatography analysis. PSSS10E6 column (length 30 cm; 0.8 cm diameter) was calibrated to 580–7,500,000 Da using molar mass polystyrene standards and had 2,6-di-tert-butyl-4-methyphenol as internal standard. The eluent used was toluene; 1 mg/mL of PGS was introduced into the GPC system at a flow rate of 1 mL/min. The eluted polymer was detected with a differential refractometer and analyzed using the PSS WinGPC scientific V6.2 software.

2.5. Development of biomimetic PGS membranes

2.5.1. Modification of the PGS surface

The approach used in this study to develop a biomimetic PGS membrane was to covalently attached the peptide sequences onto the surface of the PGS rather than just coating the surface of the membrane with the peptides. Therefore to enable and enhance this covalent binding of the peptides onto the membrane surface, modification of the PGS surface was carried out to expose hydrophilic COOH groups on its surface. The modification was done in two sequential steps of alkaline hydrolysis and acidification treatment as described below.

2.5.1.1. Alkaline hydrolysis. The alkaline hydrolysis was carried out by treating the PGS films (1 cm^2) with sodium hydroxide (NaOH) solution. As the parameters of alkali concentration used, temperature and duration of treatment have an effect on the hydrolysis outcome of the polymer, the PGS films were subjected to NaOH concentration ranging from 0.1 to 1 M and time of treatment ranging from 5 to 240 min respectively, working at 30 °C or room temperature, as detailed in Table 1. The optimal hydrolysis conditions were optimized by physicochemical analysis. Following this alkaline treatment the samples were then thoroughly washed with distilled water to remove the NaOH.

2.5.1.2. Acidification. For the acidification step the alkaline treated samples were exposed to 0.01 M HCl for few seconds. After treatment the samples were then washed thrice with distilled water.

2.5.2. Activation

For activation a solution containing 3 M 1-ethyl-3-(3-dimethylaminopropyl) carbodimide hydrochloride) (EDC) and 1 M N-hydroxysuccinimide (NHS) reagents was prepared in a pH 5 2-(*N*-morpholino)ethanesulfonic acid (MES) buffer (0.1 M). In this solution then after, the acidified PGS samples were incubated at 4 °C for 30 min under constant stirring. The samples were then statically incubated at 4 °C for another 2 and a half hours. At the end of the incubation the samples were again washed thrice with distilled water.

2.5.3. Coupling step

After the activation treatment of the PGS films, the respective peptides were covalently coupled to it. To achieve this covalent coupling the peptide sequences were dissolved in phosphate buffer solution (PBS) of pH 7.4 at a concentration of 0.5 mg/mL. The activated membranes were then incubated in this peptide solution for 16 h. Samples were finally washed thrice with bidistilled water, to remove any unbound peptides and then air dried.

2.6. Qualitative and quantitative assessments of the peptides bound to the PGS membranes

2.6.1. High performance liquid chromatography (HPLC) analysis

In order to obtain the amount of GGG-GRGDSP and GGG-YIGSR bound to the films, HPLC analysis was performed. A calibration curve was plotted by injecting known concentration of each peptide in PBS solution. The amount of peptide covalently linked to the material surface was calculated by subtracting the residual amount registered in both post-coupling and washing solutions from the initial peptide amount. Finally the peptide surface density was calculated according to the following equation:

$$density = \frac{V_i \cdot C_i - V_f \cdot C_f - V_w C_w}{A} \quad (3)$$

where C_i is the concentration of the pre-coupling solution, C_f is the concentration post-coupling and C_w is the concentration of the washing solution, V_i,V_f,V_w are the corresponding volumes and A is the area exposed to the peptide modification.

Table 1
Hydrolysis conditions in terms of hydrolysis time, temperature and NaOH solution concentration for the modification of the dense 2D films.

NaOH (M)	Temperature	Time
1	30 °C	1 h, 30 min
	room temperature	1 h
0.5	30 °C	30 min
	room temperature	1 h
0.25	30 °C	30 min
	room temperature	4 h
0.1	30 °C	30 min
	room temperature	5 min, 15 min, 30 min, 1 h, 2 h, 3 h, 4 h

The analysis system consisted of a Perkin-Elmer 200 series HPLC pump, autosampler, a C4-Alltech Prosphere HP (300A 5u, 25 cm × 4.6 mm) column and UV detector (280 nm). A mobile phase of 0.1% v/v TFA in bidistilled water (A) and 0.085% v/v TFA in acetonitrile (B) was used and a gradient elution from 30% B to 60% B for 10 min was selected. The flow rate was 1 mL/min and the injected volume was 100 μL.

2.6.2. Time-of-flight secondary ion mass spectroscopy (ToF SIMS)

The peptide functionalized PGS samples were also subjected to ToF SIMS analysis. The methodology for performing the analysis has been described elsewhere [22]. Briefly both positive and negative static SIMS measurements were performed using a ToF. SIMS 5 spectrometer (ION-TOF, Münster). The samples were irradiated with a pulsed 25 keV $Bi3^+$ liquid metal ion beam. Spectra were recorded in high-mass-resolution mode ($m/\Delta m > 8000$ at 29Si). The beam was electrodynamically bunched down to 25 ns in order to increase the mass resolution and rastered over a 500 × 500 μm^2 area. The primary ion dose density (PIDD) was kept at 5×10^{11} ions cm^{-2}, ensuring static conditions. Signals were identified using the accurate mass as well as the isotopic pattern.

2.7. Scanning electron microscopy (SEM)

The morphological analysis of PGS fabricated samples, before and after hydrolysis, was performed through a scanning electron microscope JSM 5600 (Joel Ltd., Tokyo, Japan). Before analysis, the samples were mounted on metal stubs and coated with gold to a thickness of 200–500 Å with a gold splutter.

2.8. Attenuated total reflectance fourier transformed infrared spectroscopy (ATR-FTIR) chemical imaging

The efficacy and the entity of the hydrolysis treatment performed on sample surfaces, the occurrence of the coupling reaction and the distribution of the biomolecules on the treated surfaces were investigated by ATR-FTIR Chemical Imaging. IR images of functionalized polymeric films were acquired with an infrared imaging system (Spotlight 300, Perkin Elmer) using a liquid-nitrogen-cooled 16-pixel mercury cadmium telluride line detector. The analysis was performed in the mid infrared region, 4000–720 cm^{-1}. The spectral resolution was 4 cm^{-1}. The spatial resolution was 100 × 100 μm. Background scans were obtained from a no sample region. An absorbance spectrum, resulting from 16 scans, was recorded for each pixel in the μATR mode with a penetration depth of 2–3 μm. Spectra were collected by touching the ATR objective on the sample and recording the spectrum generated from the surface of the sample. The Spotlight software used for the acquisition was also used to pre-process the spectra. Spectral images were analyzed with a compare correlation image, using as reference spectrum the most frequent one of the chemical map (the medium spectrum). The obtained

correlation map indicated the areas of an image where the spectra were most similar to a reference spectrum.

2.9. Roughness measurements

The roughness measurements of the fabricated PGS samples were carried out using a laser profilometer (UBM). The method utilized a reflection of 670 nm laser beam to determine the vertical position of the surface. 3D surface profile of the samples was recorded using a stage positioning system with maximum measurement frequency of 10 kHz. The roughness was measured on both sides of the sample and represented as average root mean square (R_a) value.

2.10. Thermal properties

The thermal properties of the polymer, i.e. glass transition temperature (T_g) and melting temperature (T_m), were studied by carrying out differential scanning calorimetry (DSC), using a Perkin Elmer DSC7 (Perkin Elmer Instrument). This analysis was carried out in order to study the effect of the hydrolysis procedure on the thermal properties of the treated materials. The amount of polymer used for the study ranged from 8 to 10 mg and was encapsulated in standard aluminum pans. All tests were carried out under inert nitrogen. The samples were heated at a heating rate of 10 °C min^{-1} between −20 and 50 °C. The test was carried out on 3 repeats of the samples. The endothermic peaks were measured with the DSC7 software.

2.11. Contact angle study

The motivation for this study is to determine if hydrophilicity and surface energy of the material change with chemical modification and peptide coating. The hydrophilicity of the PGS membranes was evaluated using static contact angle measurements. Reference liquid deionized water (4 μL) was placed on the sample by means of a gas tight microsyringe forming a drop. Photos (frame interval: 1 s, number of frames; 100) were taken to record the shape of the drops. The water contact angles on the specimens were measured by analyzing the recorded drop images using the Windows based KSV CAM software. The experiment was done on a KSV CAM 200 optical contact angle meter (KSV Instruments Ltd.).

2.12. Biocompatibility assessment — in vitro studies

2.12.1. Human cardiac mesenchymal stem cells (hC-MSCs)

Cardiac samples were obtained from auricles or myectomy of patients undergoing cardiac surgery, after Local Ethical Committee approval and signed informed consent in accordance with the declaration of Helsinki. Cell isolation was performed according to a previously reported methodology [23,24]. Briefly, myocardial fragments were minced and enzymatically digested before seeding on Petri dishes (Corning, USA) containing 10 mL of IMDM supplemented with 1% penicillin–streptomycin (P/S, Sigma, Italy) and 1% insulin–transferrin–sodium selenite (I/T/S, Sigma, Italy). After initial expansion, cells were seeded in full growth medium composed by IMDM, 10% fetal bovine serum (FBS, Sigma, Italy), 1% P/S, 1% I/T/S and 10 ng/mL basic-fibroblast growth factor (b-FGF, Sigma, Italy) for their amplification. At each passage (P), a cell aliquot was cryopreserved in a medium composed of FBS supplemented with 1% dimethylsulphoxide (DMSO, Sigma, Italy). The immunophenotypic and biological properties of these cells have been extensively documented [25]. For the present investigation, hC-MSCs from P3 to P4 were employed.

2.12.2. Rat cardiac progenitor cells (rCPCs)

rCPCs were isolated from 3 month old rat hearts according to a methodology repeatedly employed by our laboratory [26] and originally described by Beltrami et al. *Cell* 2003 [27]. In a subset of experiments of cell tracking, rCPCs were isolated from the heart of rats carrying the transgene encoding for the Green Fluorescent Protein (GFP), kindly provided by Dr Okabe [28]. Briefly, the rat heart was quickly excised from anesthetized animals and hanged by an aortic cannula to the perfusion system. The heart was dissociated with collagenase type II (Worthington Biochemical Corporation, USA) at 37 °C for 20′ and minced. After centrifugation at 300 rpm to separate cardiomyocytes, the cell supernatant was placed on Percoll (Sigma, Italy) gradient and the cell layer visualized at the interface of the desired gradient was centrifuged at 1000 rpm. Cells were resuspended in 10 mL IMDM culture medium supplemented with 1% P/S, 1% I/T/S, 10% FBS and cultured in Petri dishes (Corning, USA) at 37 °C–5% CO_2 for their amplification. c-Kit positive cells with monomorphic blast-like characteristics representing CPCs were amplified and cryopreserved. These cells have been extensively characterized in terms of stemness and multipotentiality. CPCs at P3 to P4 were employed for this study.

2.12.3. DiI cell labeling

CellTracker CM-DiI (Invitrogen, C-7001) is a DiI derivative that is somewhat more water-soluble than DiI, thus facilitating the preparation of staining solutions for cell suspensions. CellTracker CM-DiI contains a thiol-reactive chloromethyl moiety (CM) that allows the dye to covalently bind to cellular thiols. Thus, unlike other membrane stains, this label is well retained in the cells throughout several mitotic divisions and cell to cell contact does not allow dye diffusion.

rCPCs and hC-MSCs were incubated in 1–2 μM working solution for 15 min at 37 °C, and then for an additional 15 min at 4 °C. Incubation at this lower temperature appears to allow the dye to label the plasma membrane but slows down endocytosis, thus reducing dye localization into cytoplasmic vesicles. After labeling, cells were washed cells with phosphate-buffered saline (PBS), resuspended in fresh medium and used for experimental plan.

2.12.4. Cell culture on PGS membranes

PGS membranes were cut to fit exactly the size of one well of 8 well chamber slides (BD, USA). After membrane sterilization in 70% ethanol and UV exposure, DiI labeled rCPCs or hC-MSCs were counted and seeded at 15×10^3 cells/cm^2 concentration onto PGS membrane and PGS membranes containing YIGSR or GRGDSP sequences. Cell cultured in standard conditions was considered as control. Cell loaded membranes were evaluated7 days and 14 days after cell plating. Fluorescent images were digitally captured with “LAS Advanced Fluorescence” software (Leica) connected to a motorized epifluorescent microscope (Leica DMI6000B) provided by a digital camera (Leica DFC350FX) and a Z-stack automation system. Image analysis was performed with “LAS Advanced Fluorescence” software. Quantification of cell survival and adhesion was performed on photomicrographs covering the entire area of each membrane, to detect red fluorescent spots corresponding to pre-labeled cultured cells. The supernatant was carefully removed to change the medium every 2 days and to exclude from counting possible stromal fragments of dying cells. In addition, some sample was stained by DAPI to visualize nuclei. The fractional area occupied by red fluorescence and its intensity, expressed as Integrated Optical Density (IOD), were then evaluated using a software for image analysis (Image Pro Plus 4.0). All images were acquired with precalibrated gain and exposure time. Aspecific fluorescence was carried out by merging the emission signals from different excitation lengths on the same microscopic field. Due to the intrinsic limitations of cell detection on thick membranes, in some experiments, GFP rCPCs were utilized to visualize the cellular profile under specific fluorescence emission (509 nm) and the presence of DiI within their cytoplasm was assessed.

2.12.5. Scanning electron microscopy (SEM) analysis of cell seeding

In a subset of experiments, we obtained SEM images of rCPCs seeded for two weeks on PGS membrane. Briefly, after fixation on

PAF, samples were dehydrated and critically treated with 72 atm pCO_2 at 37 °C; the PGS membranes were mounted on metal stubs and coated with gold to a thickness of 60 nm with a gold splutter and analyzed by SEM (Philips SEM 501, Eindhoven, The Netherlands).

3. Results and discussion

3.1. Microstructural properties of the PGS matrices

In an attempt to develop tissue engineered cardiac patch (TECP) for the treatment of myocardial infarction, we investigated the development of PGS based matrices from two standpoints i.e. microstructural and biological. For the microstructural aspect PGS prepolymer (molecular weight, $M_w = 1.11 \times 10^3$ g/mol) was fabricated into PGS scaffolds with porosity and dense films. The PGS matrices were then surface modified and functionalized with peptides corresponding to the epitope sequence of fibronectin and laminin respectively to develop biomimetic membranes.

Human cardiac muscle is ~1 cm in thickness with a high cell density of 2×10^8 cells/cm^3 [29]. However, the generation of a thick cardiac patch (~200 μm) has been limited due to lack of vasculature in the tissue constructs [30]. Establishing stable and sustainable microvasculature in engineered tissues is of critical importance. Porous PGS scaffolds were therefore fabricated to enable exchange of nutrients and gases to the seeded cells, ultimately paving way for a sustainable microvasculature. The porous PGS scaffold prepared via salt leaching had 75% porosity. Leachate, i.e. NaCl particles of 100–125 μm range was used for the fabrication of the porous scaffolds. However morphological evaluation of the porous films via SEM, Fig. 1A–B, revealed that the films contained two different sizes of pores i.e. macropore size ranges between 20 and 50 μm and micropore size ranges between 2 and 5 μm, respectively. The small sizes of the pores in the final films could be because of the fabrication process. During the fabrication stage, the prepolymer once introduced into the salt bed is then subjected to crosslinking at 120 °C, which may lead to fusion of the salt particles leading to the final pore size distribution observed.

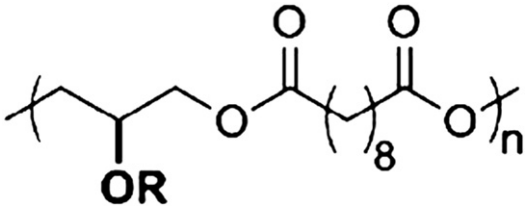

Fig. 2. Chemical structure of PGS.

As expected for the porous PGS scaffold, SEM images, Fig. 1A–B revealed that the surface of the films was not smooth. The use of the leachate and its subsequent removal had incorporated cavities and random protrusions on the surface of the films, collectively resulting in a rough surface. The R_a value for the porous PGS scaffold is 2.07 μm. The dense PGS films possessed smooth morphology (Fig. 1C) with $R_a = 0.09$ μm, on the side not in contact with the mold. However, the side in contact with the mold revealed rough parallel groove like morphology (Fig. 1D) and had a roughness value, $R_a = 0.62$ μm.

3.2. Development of biomimetic PGS membranes

PGS polymer does not possess much hydrophilic group on its carbon backbone (Fig. 2). Therefore an important prerequisite for successfully covalently binding the desired peptides on its surface is to first incorporate hydrophilic carboxylic (COOH) groups on the polymer surface. Incorporation of such COOH group will enable covalent binding of the desired peptides via amide bonding. To enable

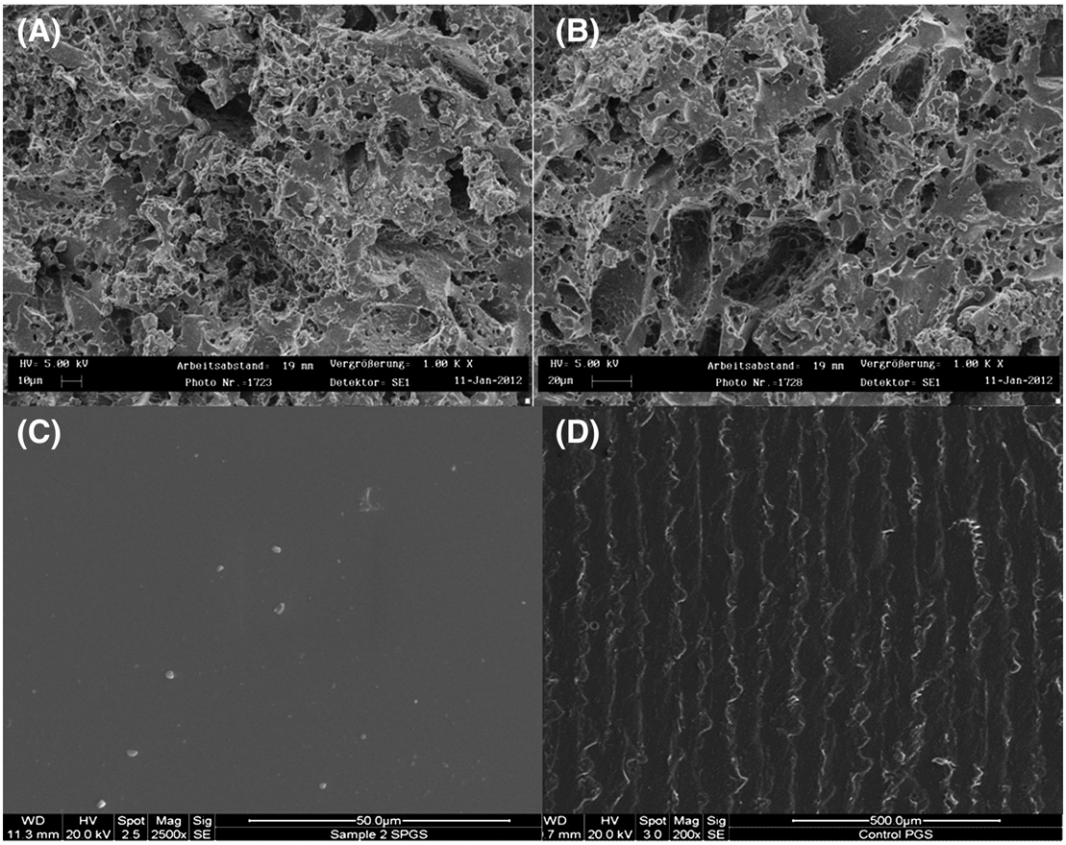

Fig. 1. SEM images of the fabricated porous scaffolds and dense films of PGS: (A) planar and (B) cross section of the porous scaffold prepared via porogen (NaCl) leaching. Planar surface of the dense PGS films with (C) smooth surface morphology and (D) rough surface morphology.

COOH incorporation, a strategy to modify the polymer was successfully developed involving sequential treatment of alkaline hydrolysis followed by acidification. The rationale of this strategy was to hydrolyze the (C═O) ester groups to COO^- carboxylate ion. These carboxylate ions, would then be converted to COOH groups during the acidification step. Another crucial step in this modification was to find optimal conditions that would incorporate the desired COOH chemical group onto the polymer without causing deleterious effect on its bulk properties. Therefore to evaluate the hydrolysis reactions, the samples were subjected to physicochemical analysis. It must be pointed out that all the preliminary investigations for optimizing the hydrolysis step were performed on the dense 2D films. Once the initial parameters were obtained the hydrolysis of the porous PGS scaffolds was then carried out.

ATR-FTIR spectra of hydrolyzed dense samples, prepared according to the conditions reported in Table 1, were acquired and compared with that of untreated PGS. This analysis was not performed on the dense samples treated by using NaOH concentration above 0.5 M and a temperature of 30 °C, since these conditions resulted in the dissolution of the samples.

The infrared spectra of all the remaining hydrolyzed samples showed the adsorption peaks due to the presence of the COO^- group at 1600 cm^{-1} demonstrating that hydrolysis occurred even under milder conditions (data not shown). The results of the ratios of the C–H band (range: 3027 cm^{-1}–2754 cm^{-1}) to C═O band (1843 cm^{-1}–1582 cm^{-1}) of the 0.1 M NaOH hydrolysed samples, which was (0.49) was the highest in comparison to that of the control (0.46) (Fig. 3B and D). The high ratio of the hydrolysed samples with respect to that of the control, indicates that an amount of (C═O) ester groups has been hydrolysed to COO^- chemical group. Chemical correlation map (Fig. 3C) also revealed the homogeneity in the presence

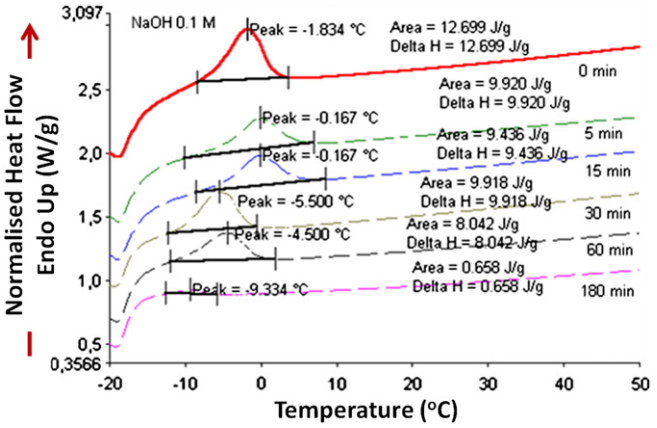

Fig. 4. Thermal profiles showing the melting temperatures and heat of fusion for the PGS films subjected to alkaline hydrolysis for different time periods.

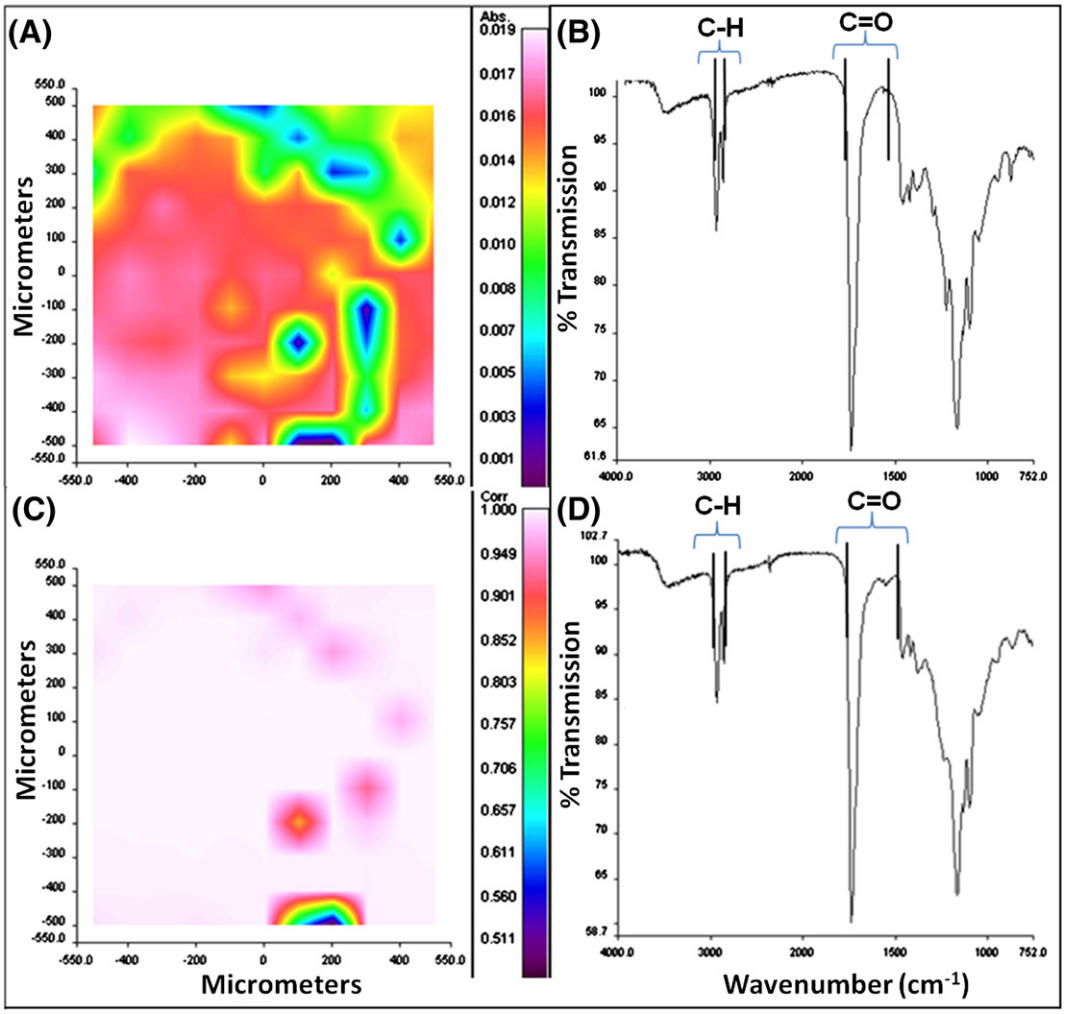

Fig. 3. The FTIR and chemical imaging spectra indicating the incorporation of COOH groups on the hydrolysed PGS membranes. (A) chemical imaging and (B) FTIR spectrum of control samples; (C) chemical imaging and (D) FTIR spectrum of hydrolysed samples.

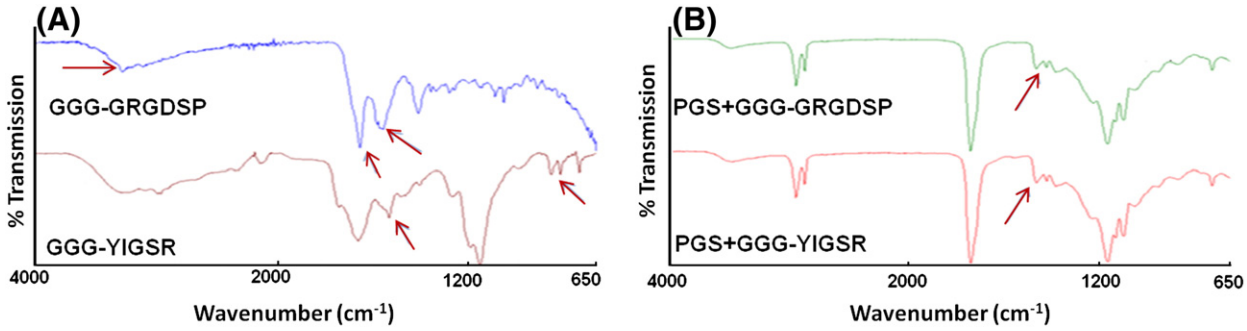

Fig. 5. ATR spectra of (A) peptide sequences and (B) functionalized PGS.

of these chemical groups (COO^-) on the surface of the membranes indicating that the hydrolysis had occurred uniformly throughout the samples. The chemical map of the control PGS film is shown in Fig. 3A. Therefore, from this chemical study, treatment of the samples with 0.1 M NaOH at room temperature was chosen.

Once the optimal concentration of NaOH for the hydrolysis was considered, the next step was to identify the optimal treatment time. This was determined by performing thermal analysis of the hydrolyzed samples using DSC. When subjected to thermal treatment, untreated PGS exhibited the transition due to the melting of the crystalline phase (T_m) at −1.8 °C, with an associated enthalpy of fusion (ΔH_f) of 12.7 J/g. A significant reduction of both T_m and associated ΔH was observed for hydrolysed samples, treated for 30 min or more. The decrease of melting enthalpy indicated a decrease in the degree of crystallinity. Although the 5 min and 15 min treatment produced a small variation of T_m and associated ΔH, when compared to the control (unhydrolysed PGS) thus indicating only a small reduction of surface crystallinity which however could promote cell adhesion [31] the 5 min alkaline treatment was chosen as this would reduce the processing time (Fig. 4).

SEM micrographs (provided as Supplementary Fig. 1) were obtained for untreated PGS and hydrolysed PGS treated according to the chosen procedure. The morphological analysis confirmed that the chosen hydrolysis condition did not produce any significant morphological modification on the surface of the sample.

Chemical, thermal and surface studies therefore confirmed that the chemical modification of the PGS membranes via alkaline hydrolysis (5 min treatment) had successfully modified the surface property of the films by incorporating more COOH chemical groups. The modification step did not seem to have deleterious effect on the bulk properties of the polymer.

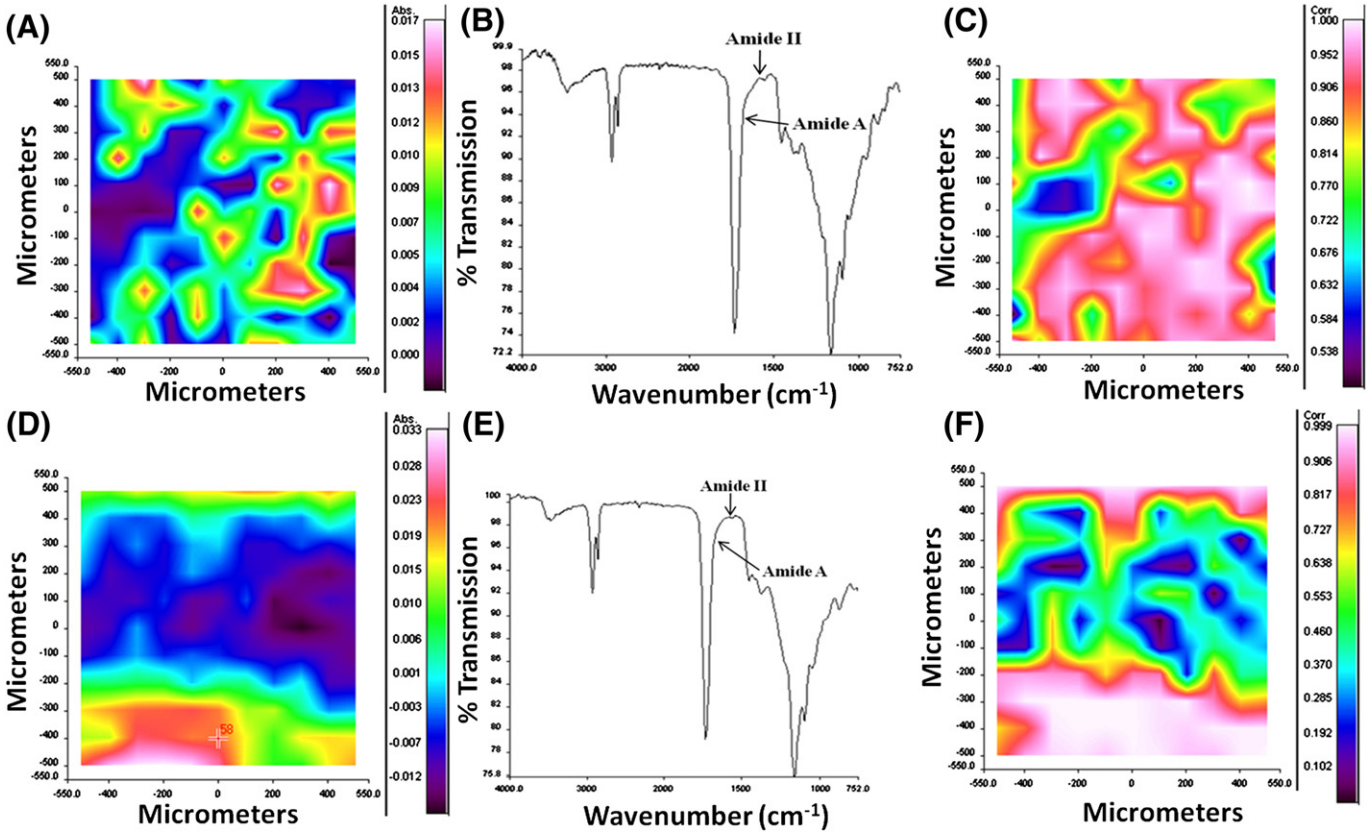

Fig. 6. Chemical maps (A and D), spectra (B and E) and correlation maps (C and F) for GGG-GRGDSP modified porous PGS (A, B, and C) and GGG-YIGSR modified porous PGS (D, E, and F).

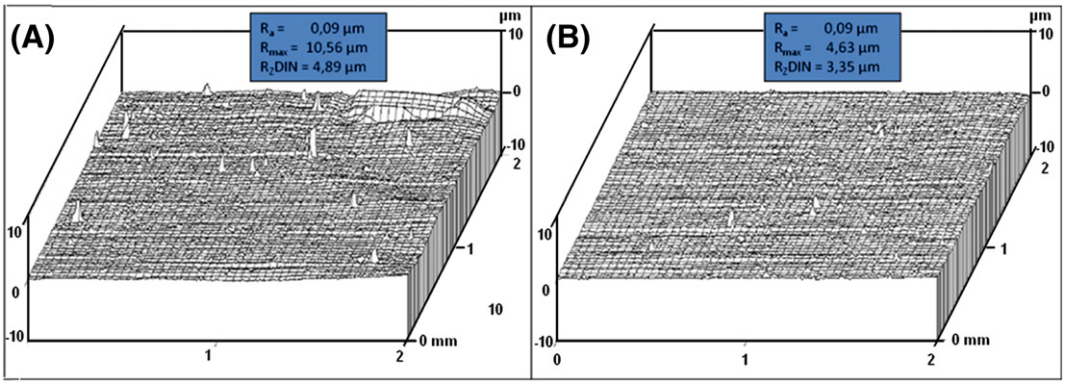

Fig. 7. Surface topography of the fabricated (A) PGS functionalized with GGGGRGDSP peptide and (B) PGS control films.

3.3. Properties of the developed biomimetic PGS membranes

3.3.1. Chemical properties

Once the hydrolysis conditions were optimized, coupling reaction with bioactive peptides was performed on PGS hydrolysed samples. ATR spectra were then acquired in order to verify the efficacy of the coupling reaction and the presence of peptide sequence on PGS functionalized samples.

In Fig. 5 the ATR spectra of GGG-GRGDSP, GGG-YIGSR, PGS modified with GGG-GRGDSP and PGS modified with GGG-YIGSR are shown. The GGG-GRGDSP spectrum was characterized by the following adsorption peaks: ν N-H = 3400 cm^{-1}; ν N-H (Amide I) = 1640 cm^{-1} and ν N-H (Amide II) = 1550 cm^{-1}. The GGG-YIGSR spectrum was characterized by the following adsorption peaks: ν N-H = 1550 cm^{-1} and ν Tyr = 723 cm^{-1}. The same characteristic adsorption peaks were detected in the spectra of functionalized samples, demonstrating the occurrence of the coupling reaction.

FTIR Chemical Imaging investigation was performed to investigate the distribution of the biomolecules on the functionalized surfaces (Fig. 6). Chemical maps were acquired from both surfaces of the PGS samples functionalized with GGG-GRGDSP and GGG-YIGSR. From the map, spectra were recorded and analyzed in order to verify the presence of the typical adsorption peaks of the peptides. In Fig. 6B, which is the magnification of spectra acquired from the chemical map in Fig. 6A, it is possible to observe the presence of a small adsorption (at 1550 cm^{-1}) related to amide II and a shoulder related to amide I. These results can confirm the presence of the GGG-GRGDSP on the sample surface. The same results were obtained for the spectra of GGG-YIGSR modified PGS (Fig. 6D and E). Correlation maps between the chemical map and the adsorption peaks in the interval of interest (1700–1400 cm^{-1} range) were therefore elaborated (Fig. 6C and F). The correlation index showed a value between 0.8 and 0.9 suggesting homogenous distribution of the peptides on the film surface.

3.3.2. Microstructural properties

No apparent differences in surface morphology of the dense PGS peptide functionalized films in comparison to the control films (nonfunctionalized) could be deduced at the micron scale level by SEM analysis (data not shown). Roughness assessment of the surfaces of peptide functionalized and control samples again ascertained what

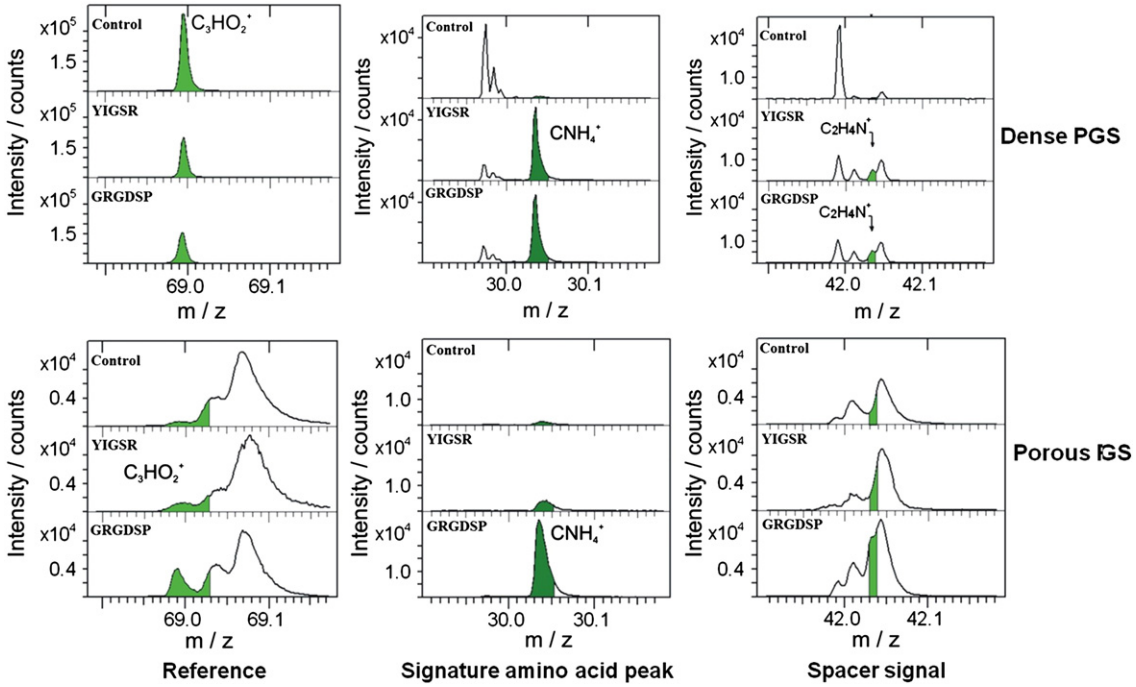

Fig. 8. ToF-SIMS spectra of PGS surfaces functionalized with GGGGRGDSP and GGGYIGSR peptides. The peaks for the reference, signature amino acid and spacer sequence observed confirmed the functionalization of the PGS surface with the respective peptide sequences.

was observed morphologically. No differences in the surface roughness of the dense PGS peptide functionalized samples ($R_a = 0.09$ μm) in comparison to the control samples ($R_a = 0.09$ μm) were observed. Fig. 7 shows the roughness of the smooth side of the PGS peptide functionalized with GGG-GRGDSP peptides and the smooth side of the PGS control films. Because of the observations made from the roughness measurements of the dense PGS peptide functionalized films, porous PGS scaffolds post peptide functionalization were not evaluated for further roughness assessment.

Surface modification of the PGS surface with peptides as expected led to a change of its wettability. Control PGS dense samples possessed a water contact angle ($\theta H_2O = 65 \pm 2$) and a total surface energy of 41.97 mN/m. The surface energy associated with a biomaterial gives an indication as to its surface polarity and how it will interface with the surrounding tissue [32]. As a general rule, as the proportion of polar groups (e.g. OOH groups) on the surface of an implant increases, the attractive forces to highly polar water molecules increase. Although the control PGS dense films were hydrophilic, incorporation of the peptides on their surface had further increased hydrophilicity with complete spreading of the water drop observed during the testing i.e. $\theta H_2O = 0^o$. On the other hand for the porous PGS scaffold, reliable contact angle measurement studies could not be carried out. This is because as soon as the water droplet was in contact with the porous surface, the droplet was absorbed due to the presence of the pores. However, similar conclusion of increased wettability of peptide functionalized porous PGS scaffold in comparison to the control can be drawn.

3.3.3. Qualitative and quantitative assessments of the covalently bound peptides onto the PGS membranes

The peptide surface density on functionalized PGS samples was determined by HPLC. The results were 60 ng/cm^2 for the GGG-GRGDSP sequence and 10 ng/cm^2 for the GGG-YIGSR sequence for the porous PGS scaffold. The dense PGS films contained 50 ng/cm^2 of GGG-GRGDSp and 65 ng/cm^2 of GGG-YIGSR.

The presence of peptides on the surface of PGS was further confirmed by the ToF-SIMS analysis as shown in Fig. 8. From the fragmentation pattern the peak at $m/z = 69$ corresponded to the substrate signal $C_3HO_2^+$. This substrate signal was chosen as the reference. Owing to the modification of the PGS surface the intensity of the substrate is the highest in the control and is seen to decrease in the modified surfaces of both the dense and the porous sample (Fig. 8). The peak corresponding to $m/z = 30$ is for CNH_4^+, which is a signature fragment of amino acids. As triple base sequence of GGG as spacer was incorporated in the peptide sequences, therefore the peak corresponding to glycine at $m/z = 42$ was also observed.

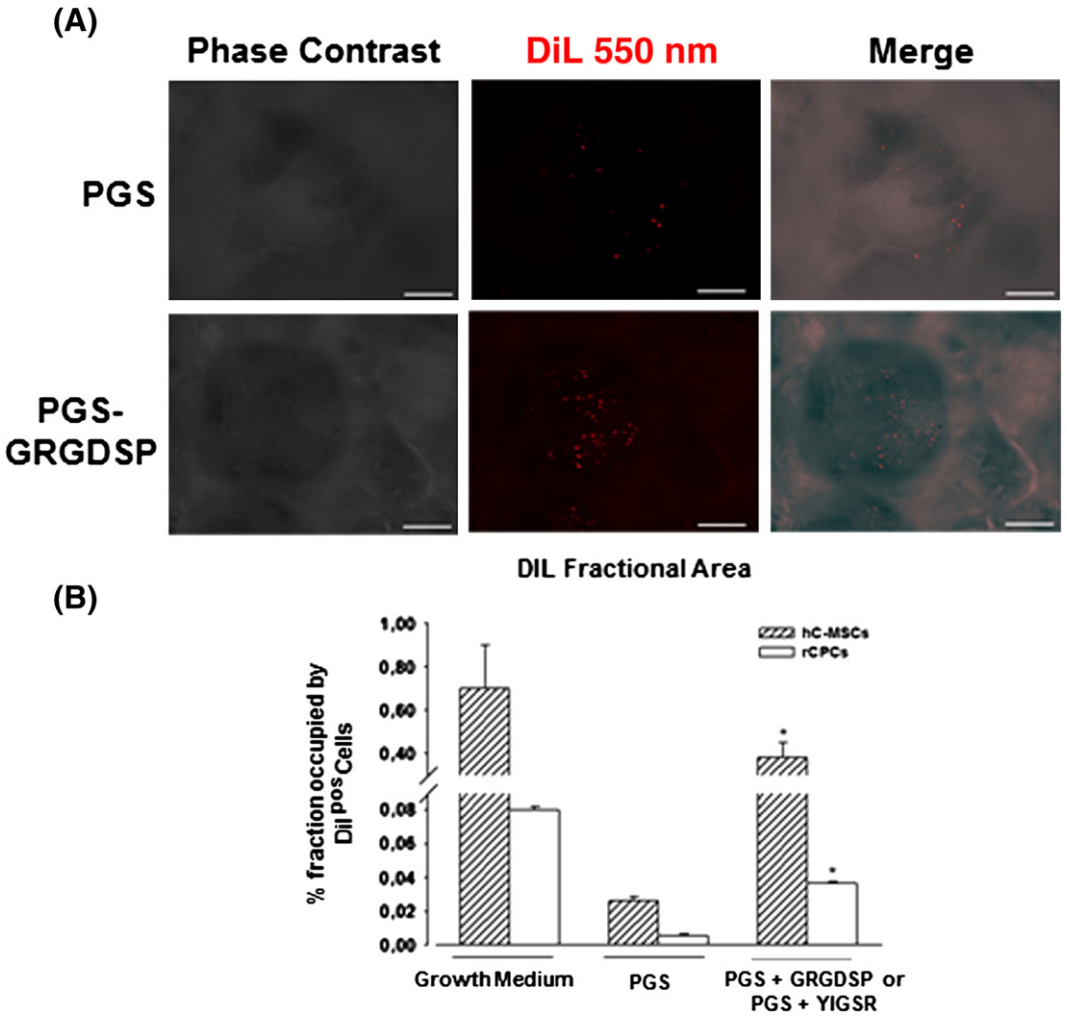

Fig. 9. A: Dil labeled hC-MSCs seeded on PGS membranes in the absence or presence of fibronectin sequence (GRGDSP) functionalization. The same microscopic field shown by phase contrast and upon fluorescence excitation is merged in the right panels. B: Quantification of the fractional area occupied by Dil labeled cells. The fluorescent signals of cells grown in the absence of PGS membranes (growth medium) are shown for comparison. Data were grouped for PGS membrane functionalization because either GRGDSP or YIGSR similarly increased the signals of Dil labeled hC-MSCs and rCPCs. The overall reduced fluorescent signals of rCPCs were likely due to their smaller size compared to hC-MSCs. Scale bars: 200 μm. * $p < 0.01$ vs PGS.

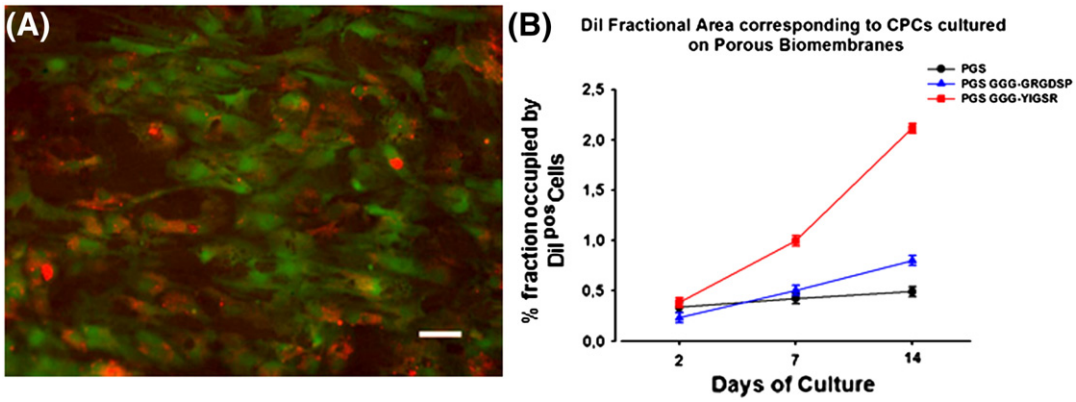

Fig. 10. A: Co-localization of green fluorescence protein (GFP, green) and DiI (red) on GFP^{pos} CPCs after two weeks of culture on PGS membranes. Scale bar = 100 μm. B: Growth characteristics of rCPCs cultured on PGS membranes. -YIGSR (red line) functionalization improves rCPC adhesion and growth compared to -GRGDSP (blue line) and control PGS membrane (black line) at 2 and 14 days after seeding. * = $p < 0.01$ vs control; ** = $p < 0.05$ vs -GRDSP.

3.4. Biological investigation of the biomimetic PGS membranes

Human and rat resident cardiac progenitors were employed as the most appropriate cellular substrate to determine the biological effects of the developed PGS matrices. rCPCs and hC-MSCs are self renewing, multipotent and give rise in vitro and in vivo to all myocardial cell compartments [9-12]. Moreover, these cells constitutively express $\alpha_4\beta_3$ integrin receptor of fibrinogen/fibrin and upon growth factor stimulation may activate $\alpha_6\beta_4$ integrin receptor of fibronectin [13]. Seeding was performed on cells labeled with CM-DiI, a membrane bound red fluorescent dye, to detect by microscopic analysis cell behavior and to allow the comparative quantification of their survival and adhesion to the surface (Fig. 9A). As expected, compared to standard in vitro conditions, the presence of PGS membranes (control samples) reduced the number of rCPCs and h-C-MSCs after 7 days of culture (Fig. 9B).

However, functionalization using GGG-GRGDSP or GGG-YIGSR sequences corresponding to the epitope sequence of fibronectin and laminin, respectively, was able to favor cell survival and adhesion to PGS biomembranes (Fig. 9A and B). The prototype of cell adhesive and bioactive matrix proteins, fibronectin has been shown to regulate cell growth, cell shape, cytoskeletal organization, differentiation, migration, and apoptosis of almost all tissue cells [9,11,33]. Laminins, a family of about 20 different heterotrimeric cross-shaped glycoproteins are the most bioactive components of basement membranes in which they assemble into a cross-linked web, interwoven with type IV collagen network [9,34,35]. Our studies therefore showed that the amount of ligand bound onto the surface of the membranes was able to promote cell adhesion and growth. In this respect, ligand surface concentration of 10^{-15} mol/cm^2 was found to be sufficient for cell spreading [36].

No significant difference was observed between RGD and YIGS sequences in these positive effects so that results were combined. Thus, 7.4-fold and 14-fold increase in area occupied, respectively, by DiI labeled rCPCs and h-C-MSCs was measured one week after plating on fibronectin and laminin peptides covalently bound to PGS membranes. To assess the effect of PGS membranes on long term growth characteristics of cardiac progenitors, DiI labeled GFP-rCPCs were

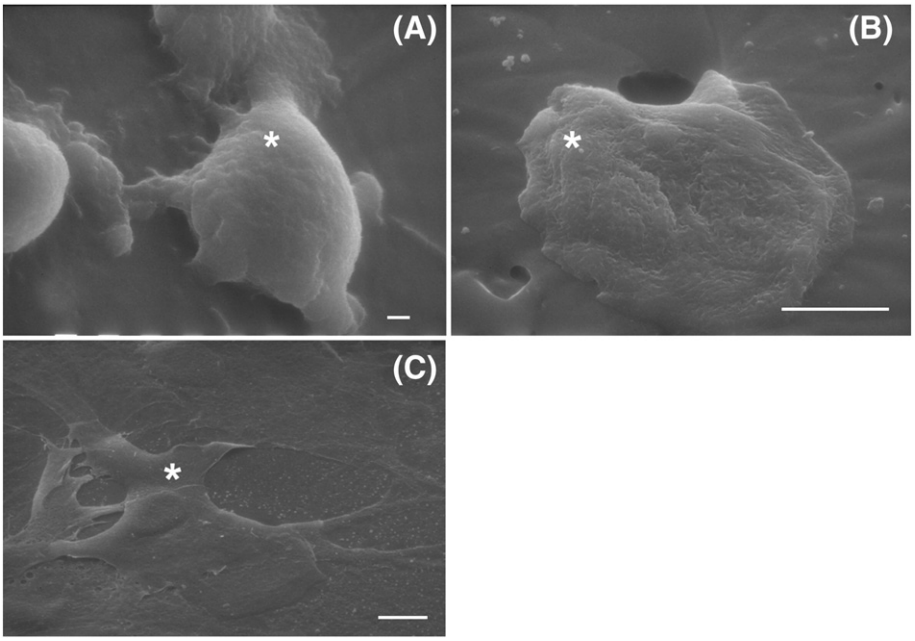

Fig. 11. SEM images of rCPCs (*) two weeks after seeding on PGS membranes. A: on a control membrane, cells show a gobular shape and adhesion is mediated only by few cytoplasmic protrusions (O.M. = 5000×; scale bars = 1 μm). B and C: rCPCs laying on -GRGDSP (B) and -YIGSR (C) functionalized PGS membranes showing cytoplasmic extension, clear formation of filopodia and cell-to-cell contact (O.M. = 2500×; scale bars = 10 μm).

examined at 48 h, 7 days and 14 days after seeding on biomimetic membranes (Fig. 10A). The study revealed that the functionalized PGS was able to support the growth of the seeded CPCs. Both GGG-GRGDSP and GGG-YIGSR functionalizations of PGS improved rCPC growth compared to control. In fact a 2-fold increase and a 5.5-fold increase in cell number were measured two weeks after plating on GRGDSP- and YIGSR-sequences, respectively (Fig. 10B).

The improved biological properties of rCPCs produced by functionalizations of PGS membranes were investigated at submicroscopic levels by SEM. On control PGS membranes, round shaped cells weakly connected to the membrane by few filopodia were observed (Fig. 11A). Both GRGDSP- and YIGSR-sequence functionalizations increased the surface accessible for cell adhesion to the membrane and promoted intercellular communication (Fig. 11B and C).

4. Conclusions

We reported the successful development of PGS matrices with microstructural features and functionalized to mimic native epitope sequences of laminin and fibronectin for cardiac patch applications. A novel strategy of surface modification of the PGS membranes was carried out by sequential treatment of alkaline hydrolysis and acid treatment without exerting adverse effect on the bulk properties of the polymer as evaluated from microstructural analysis. This chemical modification of the PGS surface ensured homogenous immobilization of the fibronectin and laminin peptide sequence, facilitated via EDC-NHS chemistry. The developed biomimetic membranes were found to be biocompatible with both rCPCs and hC-MSCs, supporting their adhesion and growth. Thus, the PGS biomimetic membranes developed hold promise to serve as carrier and delivery vehicle for functional cardiomyocytes to the infarct region of the heart.

Supplementary data to this article can be found online at http://dx.doi.org/10.1016/j.msec.2013.04.058.

Acknowledgment

We thank the technical assistance from Emilia Corradini for the SEM analysis, Jennifer Reiser for the roughness measurements and Inge Herzer for the molar mass analysis. The authors would like to acknowledge the financial support received from the EU FP-7 BIOSCENT project (ID number 214539).

References

[1] World Health Organization fact sheet on cardiovascular disease. Available from URL: http://www.who.int/mediacentre/factsheets/fs317/en/index.html 2012.
[2] R.N. Kitsis, J. Narula, Heart. Fail. Rev. 13 (2008) 107–109.
[3] R.M. Moura, A.A. de Queiroz, Artif. Organs 35 (2011) 471–477.
[4] F. Quaini, E. Cigola, C. Lagrasta, G. Saccani, E. Quaini, C. Rossi, G. Olivetti, P. Anversa, Circ. Res. 75 (1994) 1050–1063.
[5] J. Kajstura, N. Gurusamy, B. Ogòrek, P. Goichberg, C. Clavo-Rondon, T. Hosoda, D. D'Amario, S. Bardelli, A.P. Beltrami, D. Cesselli, R. Bussani, F. del Monte, F. Quaini, M. Rota, C.A. Beltrami, B.A. Buchholz, A. Leri, P. Anversa, Circ. Res. 107 (2010) 1374–1386.
[6] K.L. Christman, R.J. Lee, J. Am. Coll. Cardiol. 5 (2006) 907–913.
[7] D.L. Mann, Circulation 100 (1999) 999–1008.
[8] J.P. Vacanti, R. Langer, Lancet 354 (1999) 532–534.
[9] K. von der Mark, J. Park, S. Bauer, P. Schumuki, Cell Tissue Res. 339 (2010) 131–153.
[10] H.-W. Jun, J. West, J. Biomater. Sci. Polym. Ed. 15 (2004) 73–94.
[11] A. Mardilovich, E. Kokkoli, Biomacromolecules 5 (2001) 950–957.
[12] G. Liu, B. Hinch, A.D. Beavis, J. Biol. Chem. 271 (1996) 25338–25344.
[13] A.V. Grego, G. Mingrone, Clin. Nutr. 14 (1995) 143–148.
[14] P.B. Mortensen, Biochim. Biophys. Acta 664 (1981) 349–355.
[15] P.B. Mortensen, N. Gregersen, Biochim. Biophys. Acta 666 (1981) 394–404.
[16] Y. Wang, G.A. Ameer, B.J. Sheppard, R. langer, Nat. Biotechnol. 20 (2002) 602–606.
[17] J. Tamada, R. Langer, J. Biomater. Sci. Polym. Ed. 3 (1992) 315–353.
[18] J.M. Kemppainen, S.J. Hollister, J. Biomed. Mater. Res. A 94 (2010) 9–18.
[19] R. Rai, M. Tallawi, A. Grigore, A.R. Boccaccini, Prog. Polym. Sci. 37 (2012) 1051–1078.
[20] C.D. Pritchard, K.M. Arnér, R.A. Neal, W.L. Neeley, P. Bojo, E. Bachelder, J. Holz, N. Watson, E.A. Botchwey, R.S. Langer, F.K. Ghosh, Biomaterials 31 (2010) 2153–2162.
[21] V.L. Sales, G.C. Engelmayr Jr., J.A. Johnson, Y. Wang, M.S. Sacks, J.E. Mayer Jr., Circulation 116 (2007) 55–63.
[22] M.S. Killian, H.M. Krebs, P. Schmuki, Langmuir 27 (2011) 7510–7515.
[23] C. Frati, M. Savi, G. Graiani, C. Lagrasta, S. Cavalli, L. Prezioso, P. Rossetti, C. Mangiaracina, F. Ferraro, D. Madeddu, E. Musso, D. Stilli, A. Rossini, A. Falco, A.D. De Angelis, F. Rossi, K. Urbanek, A. Leri, J. Kajstura, P. Anversa, E. Quaini, F. Quaini, Curr. Pharm. Des. 17 (2011) 3252–3257.
[24] A. Rossini, C. Frati, C. Lagrasta, G. Graiani, A. Scopece, S. Cavalli, E. Musso, M. Baccarin, M. Di Segni, F. Fagnoni, A. Germani, E. Quaini, M. Mayr, Q. Xu, A. Barbuti, D. Difrancesco, G. Pompilio, F. Quaini, C. Gaetano, M.C. Capogrossi, Cardiovasc. Res. 89 (2011) 650–660.
[25] C. Bearzi, M. Rota, T. Hosoda, J. Tillmanns, A. Nascimbene, A. De Angelis, S. Yasuzawa-Amano, I. Trofimova, R.W. Siggins, N. Lecapitaine, S. Cascapera, A.P. Beltrami, D.A. D'Alessandro, E. Zias, F. Quaini, K. Urbanek, R.E. Michler, R. Bolli, J. Kajstura, A. Leri, P. Anversa, Proc. Natl. Acad. Sci. U.S.A. 104 (2007) 14068–14078.
[26] A. Giuliani, C. Frati, A. Rossini, V.S. Komlev, C. Lagrasta, M. Savi, S. Cavalli, C. Gaetano, F. Quaini, A. Manescu, F. Rustichelli, J. Tissue Eng. Regen. Med. 5 (2011) 168–178.
[27] A.P. Beltrami, L. Barlucchi, D. Torella, M. Baker, F. Limana, S. Chimenti, H. Kasahara, M. Rota, E. Musso, K. Urbanek, A. Leri, J. Kajstura, B. Nadal-Ginard, P. Anversa, Cell 114 (2003) 763–776.
[28] M. Okabe, M. Ikawa, K. Kiminami, FEBS Lett. 407 (1997) 313–319.
[29] M.N. Giraud, C. Armbruster, T. Carrel, H.T. Tevaearai, Tissue Eng. 13 (2007) 1825–1836.
[30] H.C. Ott, T.S. Matthiesen, S.K. Goh, L.D. Black, S.F. Kren, T.I. Netoff, D.A. Taylor, Nat. Med. 14 (2008) 213–221.
[31] L. Chou, B. Marek, W.R. Wagner, Biomaterials 20 (1999) 977–985.
[32] M. Hart, D.W. Schubert, Macromol. Chem. Phy. 213 (2012) 654–665.
[33] M. Larsen, V.V. Artym, J.A. Green, K.M. Yamada, Curr. Opin. Cell Biol. 18 (2006) 463–471.
[34] H. Colognato, P.D. Yurchenco, Dev. Dyn. 218 (2000) 213–234.
[35] J.H. Miner, P.D. Yurchenco, Annu. Rev. Cell Dev. Biol. 20 (2004) 255–284.
[36] S.P. Massia, J.A. Hubbell, J. Cell Biol. 114 (1991) 1089–1100.